

Attrition of particulate materials in a conventional spouted bed

Robson C. de Sousa¹, Fábio B². Freire & José T. Freire²

¹ Department of Rural Engineering, Federal University of Espírito Santo - UFES, Alto Universitário, S/N°, Guararema, CEP 29500-000, Alegre, ES, Brazil.

² Department of Chemical Engineering, Federal University of São Carlos - UFSCar, Rodovia Washington Luiz, km 235, SP-310, CEP 13565-905, São Carlos, SP, Brazil.

Abstract: - In this study, attrition of spherical materials (glass and alumina) and non-spherical materials (dolomite particles) in a spouted bed was evaluated through experimental and numerical results. The experiments were carried out using a cone-cylinder spouted bed. The operating conditions used were: air inlet velocity of 1.10 and 1.20 u/u_{ms} and operating time of 2250 minutes. Two mathematical models were applied to describe the attrition of the materials used. The experimental results showed that attrition reduced the mass and size of the alumina spheres and dolomite particles. The increased air inlet velocity promoted greater attrition of the alumina spheres. Regarding the fluid dynamic performance, attrition had an influence on the parameters: minimum spouting velocity and maximum pressure drop. Only one of the proposed models presented predictions consistent with and close to the experimental data obtained in this work.

Keywords: - Attrition, spouted bed, particulate materials

I. INTRODUCTION

The spouted bed has been widely used in various physical and chemical applications involving solid-fluid contact, such as drying [1,2], coating [3], granulation [4], gasification [5,6], combustion [7] and pyrolysis [8,9]. This is due to the high mass and heat transfer rates that are reached during the cyclical movement, which is responsible for the achievement of an efficient degree of fluid-particle contact, especially if coarse particulate materials ($d_p > 1\text{mm}$) are used [10-13]. The cyclical movement starts when a fluid, usually an air current, is injected through an orifice located at the lower end of the conical region at a flow rate that is sufficient to promote the upward motion of the particles, forming a channel in the center of the conical region (spout region). The particles reach a maximum height (the fountain region) and return close to the wall of the spouted bed in the countercurrent direction (annular region). The particulate matter can return to the spout region through the spout-annulus interface; however, the highest incidence is verified at the base of the spouted bed. Therefore, the particulate material reverses its moving direction and is, again, transported upwards [10-13].

The particulate material is subjected to intense contact by the air flow rate, especially when it is moving through the spout and fountain regions [10]. In these regions, collisions happen more frequently than in the annular region of the bed [14], which may lead to attrition of the particulate material and, thus, to the reduction of its size and to the emission of "fine" particles, which need to be separated at the end of the process most of the time [15]. The literature has shown that attrition mostly occurs in the spout region due to the high velocity reached by the particulate material, promoting intense collisions between particles and of particles against the solid wall which forms the spout channel. In the fountain region, besides collisions, there is also the impact of particles against the wall of the spouted bed [14]. Attrition depends on a number of factors such as the properties of the solid material (porosity, specific surface area, mass, shape, etc.) and operating conditions (air inlet velocity, temperature, etc) [14,15].

Several studies have investigated the effects of attrition and of what may influence it during the processing of solid materials in the spouted bed. Mathur and Epstein [10] reported that performance parameters such as cone angle, bed depth and inlet gas velocity are factors which have a significant influence on attrition. Flamant et al. [17] observed that the amount of fine materials of calcite collected at the exit of the cyclone increased with an increased air inlet velocity; Massarani et al. [18] found that the production rate of annatto powder obtained from attrition increased when greater bed heights were used; Al-Senawi et al. [19] noticed that by increasing the diameter of the inlet nozzle of the bed, attrition of the polymers used in the experiments also increased; Fernández-Akarregui et al. [14] showed, through experimental data, that attrition was responsible for reducing the mass and size of the grains of sand, as well as influencing the dynamics of the bed.

Despite the studies performed, the literature still lacks information on attrition in a spouted bed, once there are a variety of particulate materials with quite distinct specific properties and different morphological structures available for use. Moreover, the spouted bed may have several configurations and dimensions; thus, each spouted bed has a specific range of operating conditions as a function of its configuration. This difficulty also refers to the numerical approach, since most mathematical models have been applied to predict the attrition

of solid materials in fluidized beds [20,21]. In light of this context, this study aimed to analyze the attrition of spherical and non-spherical materials from experimental data and correlation as a function of time and also of air inlet velocity in a spouted bed. Regarding the correlation data, the models used were those proposed by Gwyn [21] and Lee et al. [20], which take mass loss throughout time into consideration.

II. MATERIALS AND METHODS

2.1 MATERIALS AND EQUIPMENT

Table 1 shows particulate materials, physical properties and techniques of measurements.

Table 1 - Particulate materials, physical properties and techniques of measurements.

Properties	Glass	Alumina	Dolomite
d_p (mm)	3.2 (a)	3.0 (a)	6.22 (b)
ρ_{ap} (kg/m ³)	-	1501 (c)	-
ρ (kg/m ³)	2500 (d)	2482 (c)	2819 (c)
Φ (-)	1 (e)	1 (e)	0.85 (b)

(a) Sieving, (b) Image analysis, (c) Pycnometry gas, (d) Pycnometry liquid and (e) Narimatsu [23].

The schematic diagram of the experimental apparatus used to collect the attrition data is shown in Figure 1. The spouted bed is composed of a conical base (internal angle 60°) of height of 0.20 m, inlet orifice diameter of 0.03 m, a cylindrical column with height of 1.20 m and diameter of 0.30 m. For all tests, the mass of these particulate materials added into the conical base is fixed at 2.6 kg. The pressure data were collected using two pressure transducers, one to measure the air velocity in the orifice and the other to measure the bed pressure drop. Data of pressure was collected every 30 seconds by the acquisition system; 1024 points at a frequency of 500 Hz are captured. These data were then addressed, filtered and processed using a microcomputer data acquisition system including signal conditioning, data acquisition modules and LabVIEW® software.

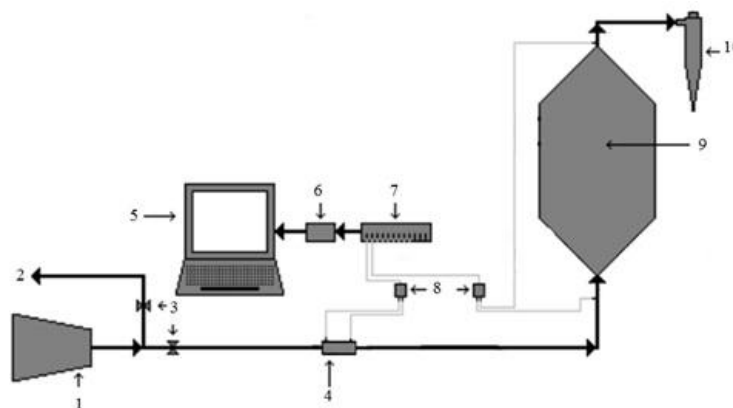


Figure 1: Schematic diagram of the experimental apparatus. Details: 1 – blower; 2 – by pass system; 3 – valves; 4 – venturi; 5 – computer; 6 – data acquisition board; 7 – signal conditioner; 8 – pressure transducers; 9 – spouted bed; 10 - cyclone.

2.2 EXPERIMENTAL PROCEDURE

The particle size distribution was determined by sieving and the Sauter average diameter was calculated according with the Equation 1.

$$dp = \frac{1}{\sum \frac{x_i}{dp}} \quad (1)$$

Pressure drop curves as a function of increased and decreased air surface velocity were built by using the methodology proposed by Mathur and Epstein [10]. For the attrition trials, air velocity was kept constant for an operating condition at a given time interval. At the end of experiments, the valve of the excess air discharge pipe was fully open and the blower was turned off. With the system completely off, the particulate materials were removed through the conical region of the spouted bed and, then, they were weighed on a digital scale with an accuracy of 0.001g. When it comes to the alumina spheres, it was necessary to dry them in a forced convection oven for 24 hours, due to rapid adsorption of moisture during the operation. Attrition was quantified by mass loss (X_a) according to Equation 2, where M_i is the mass of the solid at time (t) and M_0 is the initial mass of the solid.

$$X_a = \left(1 - \frac{M_i}{M_0} \right) 100 \quad (2)$$

The models used to predict attrition were the ones from Gwyn [21] and Lee et al. [20], which consist of equations 3 and 4 shown in Table 2.

Table 2: Mathematical models proposed by Gwyn [21] and Lee et al. [20]

$Rt = kp m t^{m-1} W$	Gwyn [21] (3)
$We = (W_0 - W_{min}) e^{-k_a t} + W_{min}$	Lee et al. [20] (4)

In relation to the model proposed by Lee et al. [20], the constant k_a was obtained through the method adopted by Fernández-Akarregui [14], which considers the minimum spout velocity as shown in Equation 5.

$$k_a = k_0 e^{-k_1 / u_0 (u_0 - u_{ms})} \quad (5)$$

The model parameters were estimated based on computer routines developed in the Matlab® software. In order to do so, the criterion used was the minimizing of squared deviations between experimental data and data predicted by the models.

III. RESULTS AND DISCUSSION

Figure 2 shows the particle size distribution curves for the glass beads under conditions of stable spout ($u/u_{ms} = 1.10$ and $u/u_{ms} = 1.20$) for the time of 2250 minutes. For the operating conditions employed, attrition of the glass beads was not verified, since the mass of the particulate bed remained the same until the end of the experimental trials. The mean diameter calculated before and after the time of 2250 minutes was 3.17 mm. Therefore, for the time employed, there was no wear of the particles used.

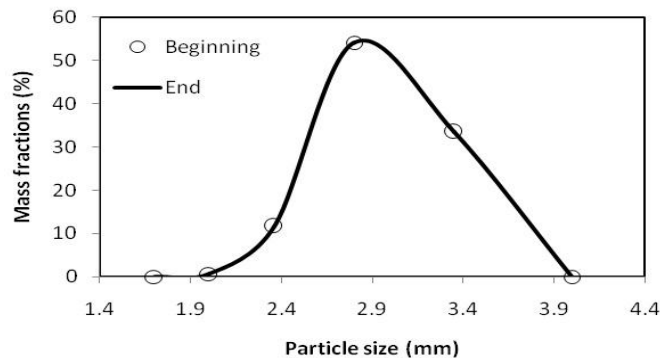


Figure 2: Particle size distribution curves of glass spheres at the beginning and end of the test attrition.

3.1 EFFECT OF POROSITY AND AIR VELOCITY

Figure 3 shows the data related to mass reduction and attrition evolution as a function of time for the alumina spheres for $u/u_{ms} = 1.10$ and 1.20 at the attrition period of 2250 minutes. It is observed that the mass of alumina spheres decreased with increased time from 2.6 kg to 1.85 kg using the lowest air velocity and from 2.6 to 1.95 ($u/u_{ms} = 1.20$) for the highest condition. For both situations, this reduction can be considered significant, taking into consideration the amount of mass of alumina spheres used in the beginning of the experiments (2.6 kg). This can be observed in Figure 3, since the attrition data (X_a) are, approximately, 28% for $u/u_{ms} = 1.10$ and 24% for $u/u_{ms} = 1.20$.

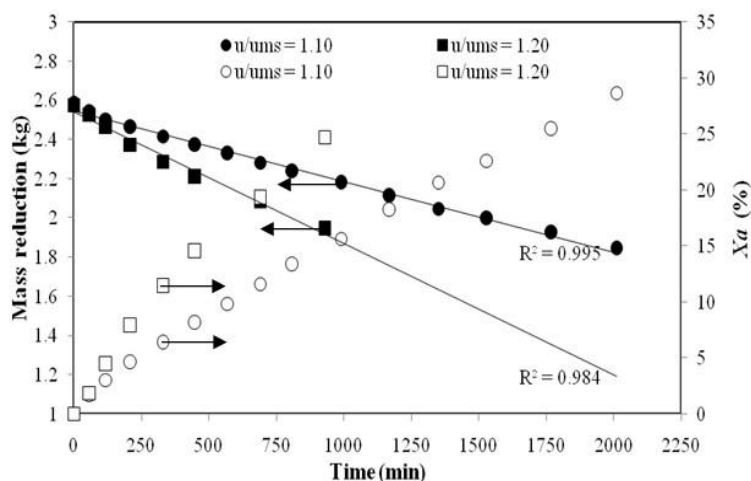


Figure 3: Experimental data for mass reduction of the alumina spheres as a function of time and evolution attrition.

In Figure 3, except for the three initial points, it can be considered that there was a linear reduction, once the value of R^2 for the experimental data obtained was 0.99. The behavior observed in the initial moment suggests that it is a specific characteristic of moving beds, especially in the case of fluidized and spouted beds. This is due to wear that happens because of surface abrasion, which is one of the ways attrition can occur, and not due to the breaking in smaller particle sizes (fragmentation).

According to Fernández-Akarregui [14], it is widely accepted that the attrition of particulate materials be evidenced by successive collisions between particles and the physical boundaries within the spouted bed. Surface abrasion is higher in the spout region, especially because, in this region, the velocity of solid materials and the contact between particles and the wall formed by the spout-annulus interface are high. On the other hand, collisions are more frequent in the fountain region and occur when the contact among particles and between particles and the wall of the spouted bed happens. In this case, impact intensity depends on many factors, especially on the number of collisions, surface area of the particulate material and particle velocity. The specific properties of the solid materials also have to be taken into consideration.

In the specific case of the alumina spheres, it can be observed that, due to the fact that it is a porous material, probably, resistance to friction was lower and, because of that, attrition was very considerable. According to Bemrose and Bridgwater [16], this happens as a result of surface abrasion, which means the breaking of the surface of solids, which is exposed to contact, into very “fine” particles. Therefore, as the particle surface is worn, it becomes smaller compared to its original size, and its weight also decreases. This helps explain the reason why the glass beads resisted to friction inside the spouted bed, making it possible to infer that the operating conditions employed in the experimental trials, as well as the fact that it is a non-porous material, contributed to the non-occurrence of attrition.

Another detail lies in the time used for the experimental trials in this study. It was not possible to evaluate if the mass decrease would continue to be linear for periods of time over 2250 minutes. Despite the porosity of the alumina spheres, it was expected that attrition would not be significant from a given time interval to the point of considering mass to be constant for the operating conditions used. This was verified by Lee et al. [20], who analyzed attrition of a type of porous adsorbent. These authors observed that the mass of adsorbent did not show significant decrease after 15 hours of operation. Longer periods of time were reached with grains of sand, in which case over 200 hours, depending on the air velocity used in the experimental trials, as observed in the study performed by Fernández-Akarregui [14]. For this reason, it is believed that the linear mass reductions observed in Figure 3 may be associated with the time employed in the experimental trials, which was

not enough for the steady state to be reached. Nonetheless, for the drying of pastes in a spouted bed, 2250 minutes were enough.

When it comes to air velocity, it can be verified that for the highest air inlet velocity ($u/u_{ms} = 1.20$), mass reduction is more pronounced. It can be noticed that there is a significant difference between the points which correspond to the highest and lowest velocities used in the experiments. This effect is due to the amount of kinetic energy that is transferred from the air drag force to the alumina spheres, which becomes higher when air inlet velocity increases. Once the kinetic energy of the alumina spheres increased, the interparticle collisions and the impact with the wall of the equipment became more frequent; consequently, attrition increased during the cyclical movement of the particulate material inside the spouted bed; hence, mass losses were evidenced.

Figure 4 presents the particle size distribution for the alumina spheres showing that the size of the material decreased, since the mean diameter found previously corresponded to 3.42 mm, whereas at the end of attrition it was 3.09 mm.

It is also observed that the larger particles tend to become smaller when compared to smaller-sized particles. A possible explanation for this situation is related to the particle size, once, according to Fernández-Akarregui [20], the probability of small particles to wear is lower, since small particles have few structural flaws or imperfections when compared to larger particles, thus, they are more resistant to friction; therefore, attrition becomes lower.

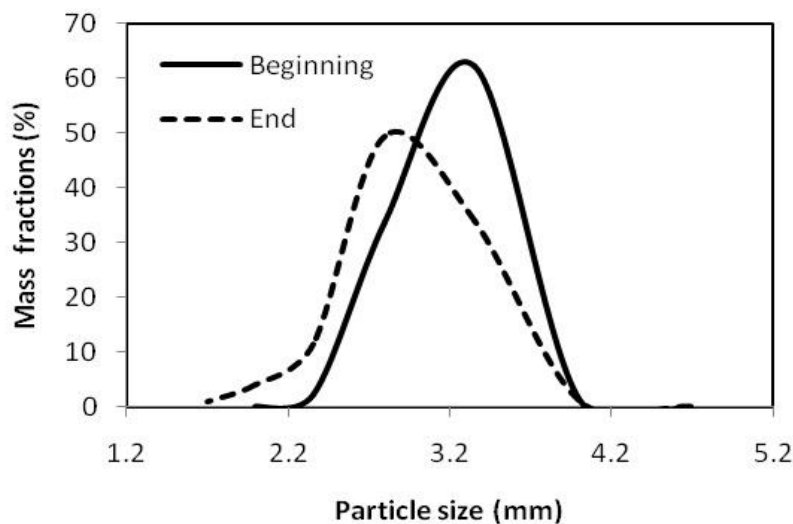


Figure 4: Particle size distribution curves of alumina spheres at the beginning and end of the test attrition.

3.2 ATTRITION IN NOM-SPHERICAL PARTICLES

Figure 5 show the data obtained for the bed mass and for evolution of attrition as a function of time for the dolomite particles. It can be verified that from the initial load of solids, 2.6 kg, there was a decrease in mass of the dolomite particles with time until the mass of 1.60 Kg was reached at the end of attrition. However, it can be seen that the attrition of the dolomite particles and the decrease in mass are inverse behaviors, being the value of 37.5% reached.

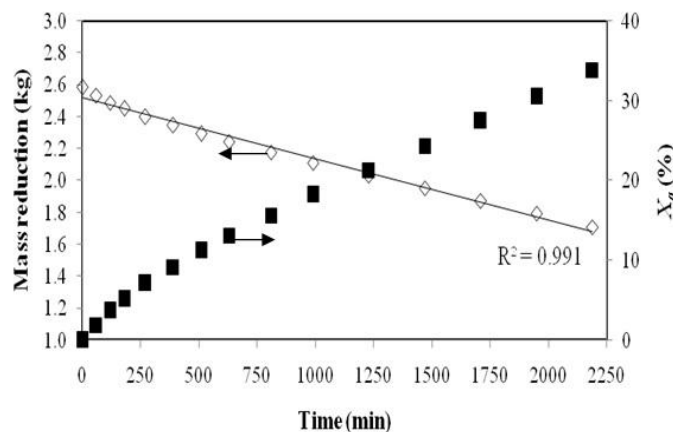


Figure 5: Experimental data for mass reduction of the dolomite particles as a function of time and evolution attrition.

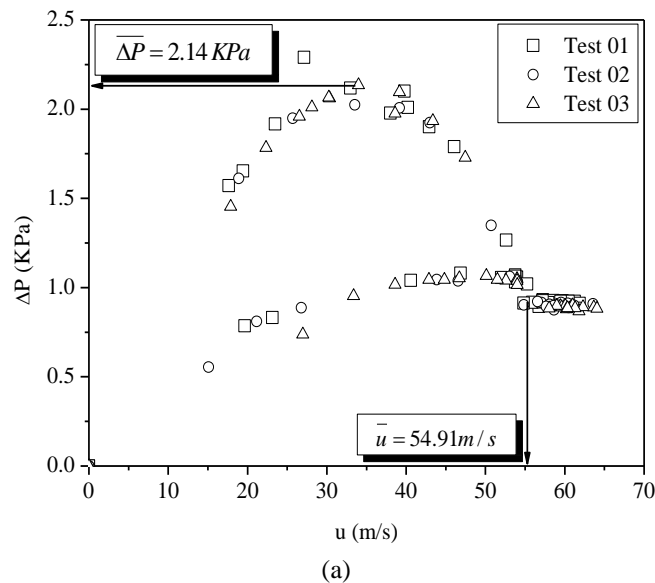
The behavior observed in Figure 5 was similar to what was observed for the alumina spheres shown in Figure 3. The same can be said in relation to the tendency followed by the first three points of each curve that shows a non-linear mass decrease when compared to the other points. This fact contributes to confirm what was previously suggested, where it was stated that there is intense contribution of the operating conditions and of the properties of the material, especially the irregular shape of particles. For this type of material, morphological structure should be taken into consideration, once they are solid materials formed by peaks or edges which, when subjected to impact, wear out quickly tending to become rounded, as shown in Figure 6, justifying why attrition was so severe exceeding 35% of the initial mass value.



Figure 6: Images of dolomite particles before and after attrition

3.3 EFFECT OF ATTRITION IN FLUID DYNAMIC BEHAVIOR SPOUTED BED

Figures 7 and 8 show the data for pressure drop as a function of air inlet velocity. Figures 7a, 7b, 7c and 7d show the characteristic curves for the alumina spheres for different periods of time in the process of attrition: 0, 210, 690 and 2250 minutes, respectively. It can be stated that data are reproducible, since the deviations for the beginning and end of the experiments are within the range of experimental error (< 5%). Based on the behavior presented, it was determined that all characteristic curves exhibit the typical behavior of a conventional spouted bed as proposed by Mathur and Epstein [10].



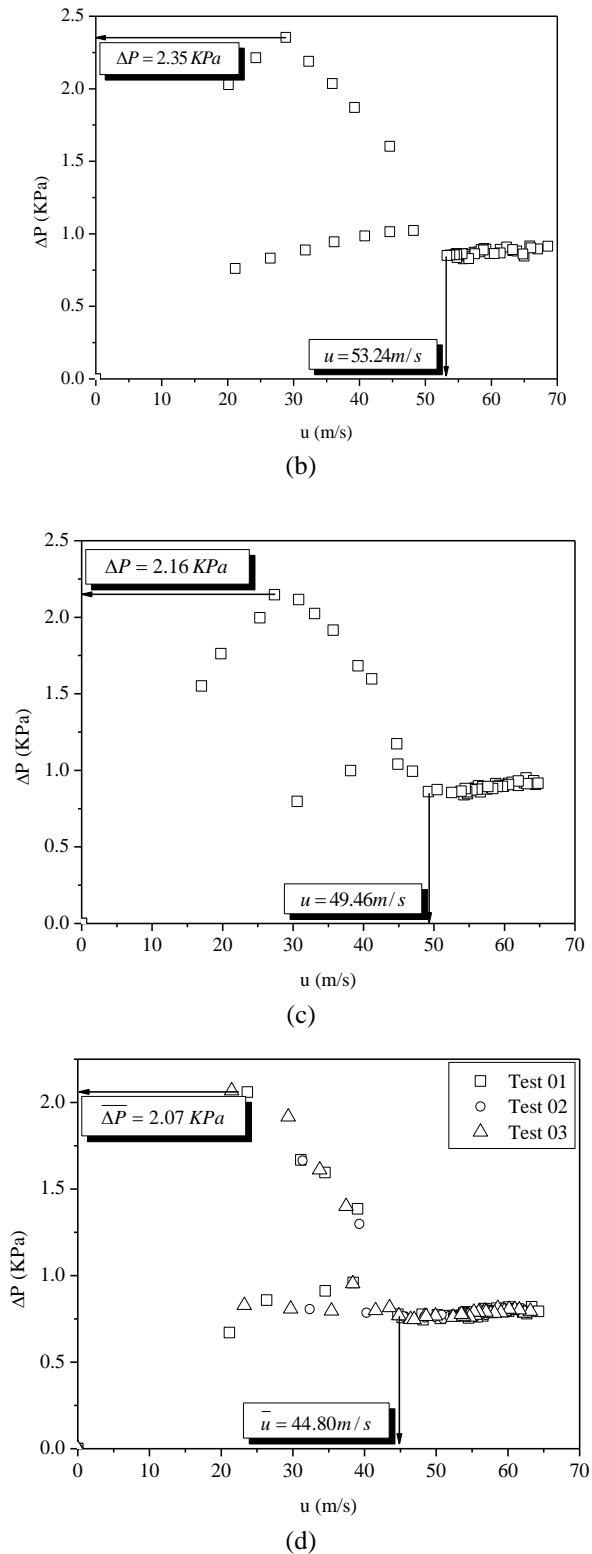


Figure 7: Pressure drop as a function of air velocity (alumina spheres in the time: (a) 0 minute; (b) 210 minutes; (c) 690 minutes e (d) 2250 minutes).

Table 3 shows maximum pressure drop (ΔP_{max}), minimum spouting velocity, (u_{ms}), time and attrition quantified in percentage terms. Through the data presented in this table, it was observed that significant decrease in the minimum spouting velocity occurred after attrition, approximately 17% compared to the value of velocity at $t = 0$.

Table 3: Data for maximum pressure drop, minimum spouting velocity, mass alumina spheres and attrition.

Figure	Time (min)	ΔP_{max} (kPa)	u_{ms} (m/s)	Mass (kg)	X_a (%)
a	0	2.14	54.91	2.58	0
b	210	2.35	53.24	2.46	4.57
c	690	2.16	49.46	2.28	11.62
d	2250	2.07	44.80	1.75	32.07

For the dolomite particles, the curves presented behaviors similar to what was observed for the alumina spheres. For this reason, Figures 8a and 8b only show the characteristic bed curves for the dolomite particles referring to the beginning and end of attrition (0 and 2250 minutes, respectively).

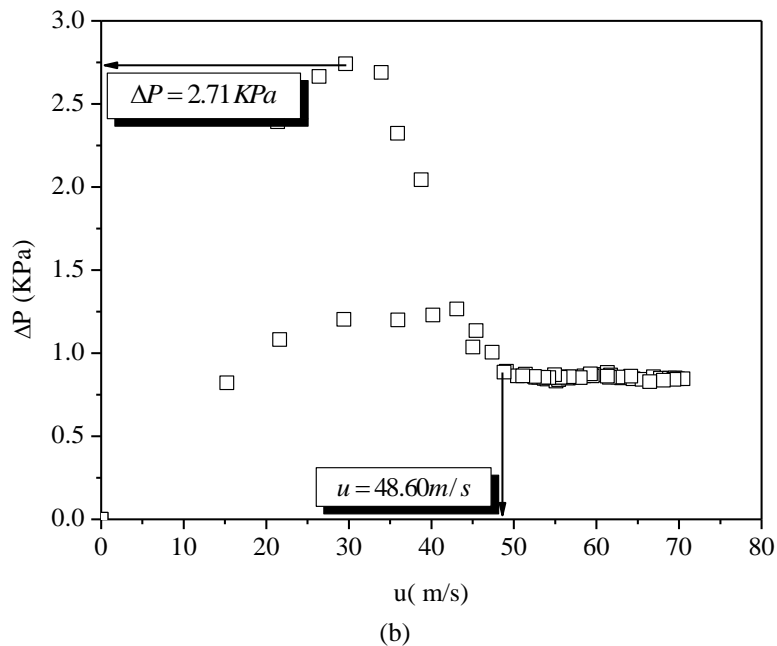
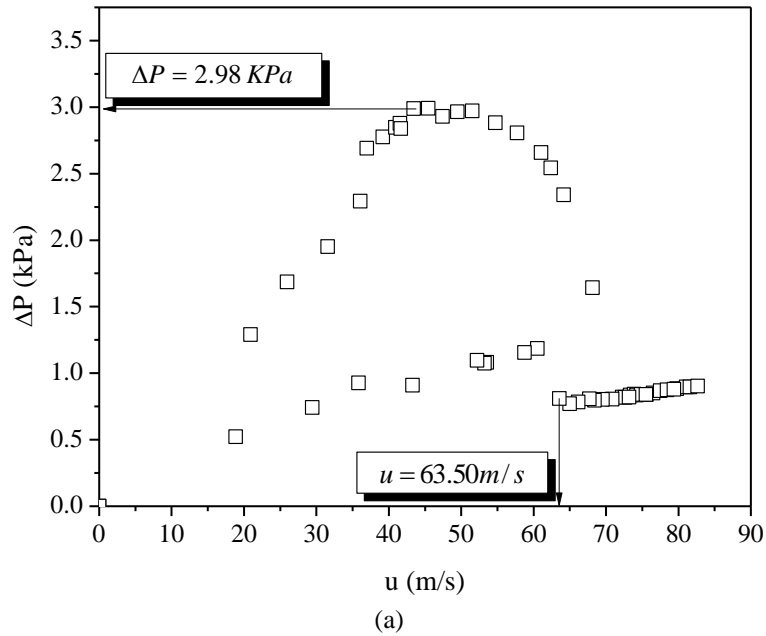


Figure 8: Pressure drop as a function of air velocity (dolomite particles in the time: (a) 0 minute and (b) 2250 minutes).

The values of maximum pressure drop (ΔP_{max}), minimum spouting velocity (u_{ms}), mass and time of attrition are shown in Table 4.

Table 4: Data for maximum pressure drop, minimum spouting velocity, mass of dolomite particles and attrition.

Figure	Time (min)	ΔP_{max} (kPa)	u_{ms} (m/s)	Mass (kg)	X_a (%)
a	0	2.98	63.50	2.58	0
b	2250	2.71	48.60	1.61	37.4

By analyzing the results shown in Table 4, it can be observed that the behavior of dolomite is similar to what was noticed for the alumina spheres; that is, a decrease was verified in both the minimum spouting velocity and mass of the dolomite particles as a function of time.

According to German [22], the morphological particle structure may alter the packing condition of solid materials, since the further a particle is from the spherical shape, the lower is its porosity as well as is the packing density of a distribution that contains it. Since the dolomite particle is a solid material of irregular shape, theoretically, porosity is low for a bed which is composed of non-spherical particles. For this reason, the minimum spouting velocity, condition which is necessary to keep the spouting stable, becomes lower at the end of attrition, where particles are more rounded.

Concerning the maximum pressure drop, an increase in this parameter up to a certain point followed by a decrease, which corresponds to the end of attrition, were noticed for both types of particulate materials used as can be seen in Tables 3 and 4. It is believed that this behavior is related to a joint action of two factors, mainly for the dolomite particles. These factors are the way the particles settle in the conical region and the mass concentration of particles in the spouted bed, and they are affected by attrition and by the cyclical movement of the particulate bed inside the spouted bed.

It is also observed that the maximum pressure drop of the dolomite particles is larger in comparison with the data obtained for the alumina spheres. A possible explanation for this fact is the physical properties of materials, which are very distinct, especially specific mass. Thus, for a higher specific mass, the pressure drop became higher.

3.4 MODEL PREDICTIONS

The results obtained by the attrition models adjusted to the experimental data are shown in Figure 09 for the alumina spheres under operating conditions of initial mass load of 2.6 kg and $u/u_{ms} = 1.10$ and 1.2. Figure 10 shows the results for the dolomite particles under operating conditions of initial mass load of 2.6 kg and $u/u_{ms} = 1.10$.

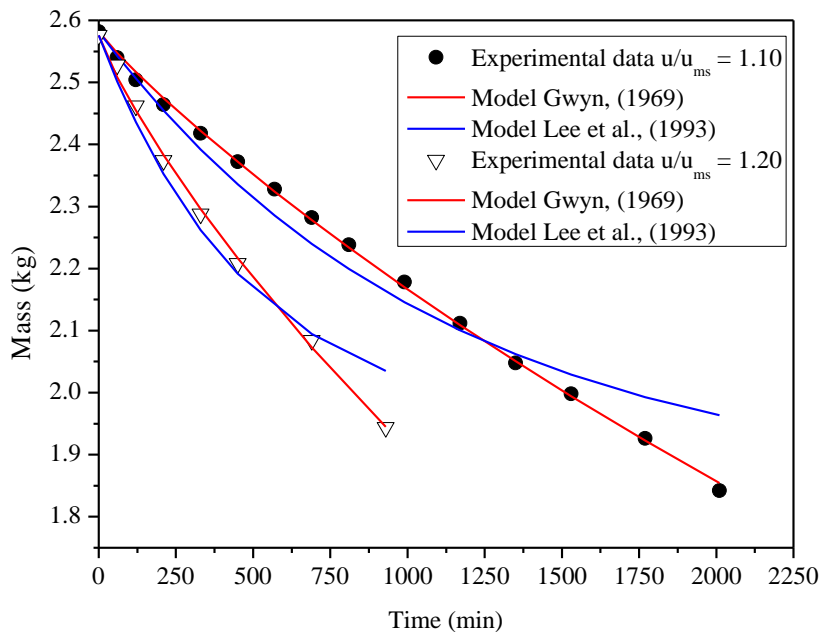


Figure 9: Mass reduction alumina spheres as a function of time. (Points: experimental data; lines: calculated).

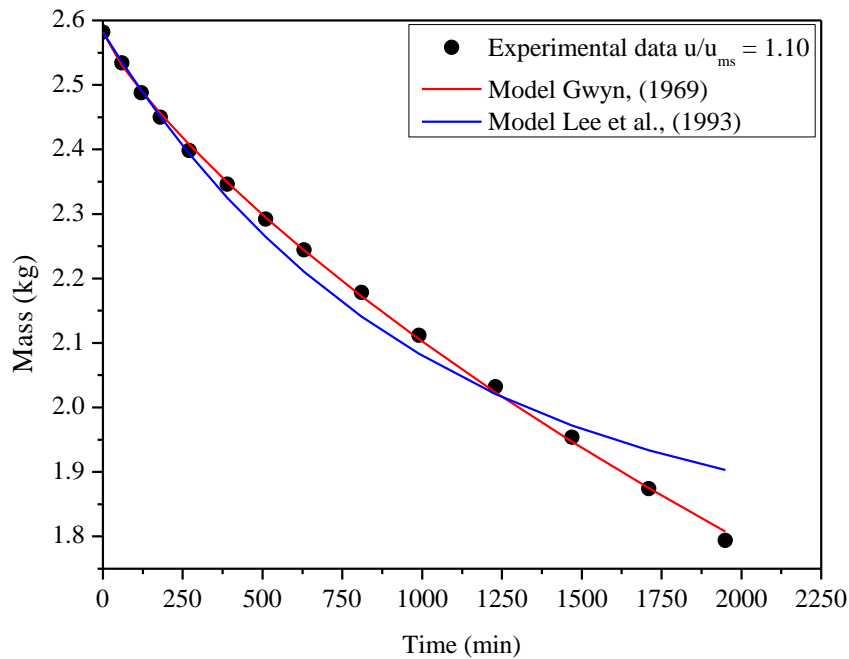


Figure 10: Mass reduction dolomite particles as a function of time. (Points: experimental data; lines: calculated).

As shown in Figure 09, the model proposed by Gwyn [21], provided the best adjustment to the experimental data for both alumina spheres and dolomite particles. Table 5 shows the values of the m and k_p parameters estimated in the attrition of alumina spheres and dolomite particles.

Table 5: Parameters m e k_p (model Gwyn [21]).

Materials	u/u_{ms}	m (-)	k_p (s^{-m})
Alumina spheres	1.10	0.91	$3.61 \times 10^{-004} s^{-m}$
Alumina spheres	1.20	0.86	$9.01 \times 10^{-004} s^{-m}$
Dolomite particles	1.10	0.82	$8.43 \times 10^{-004} s^{-m}$

Although the model proposed by Lee et al. [20] did not present satisfactory results between experimental and predicted data, the phenomenological behavior is consistent with attrition kinetics, as seen in the literature. In this case, it is observed that the particulate material mass decreases exponentially with time. Table 6 shows the k_0 and k_1 parameters estimated to determine the k_a constant of the model.

Table 6: Parameters k_0 e k_1 (model Lee et al. [20]).

Materials	k_0 (s^{-1})	k_1 (m^2/s^2)
Alumina spheres	5.56×10^{-4}	- 4.42
Dolomite particles	1.0×10^{-3}	4.42

IV. CONCLUSIONS

It can be concluded that it was possible to analyze attrition of glass beads and dolomite particles in a cone-cylinder spouted bed through both experimental trials and the numerical models used. Regarding the glass beads, it can be stated that, for the operating conditions employed in the experiments, this material resisted attrition and, thus, its diameter size did not decrease. The alumina spheres and dolomite particles presented linear decreases in mass as a function of time. Besides that, it was observed that decrease in size of the alumina spheres was more pronounced when the highest air inlet velocity was used. Attrition of both materials had an influence on the fluid dynamic performance of the spouted bed, altering fluid dynamic parameters, mainly the minimum spouting velocity. The mathematical models used showed consistent results, contributing to the understanding of attrition in a spouted bed; however, the model proposed by Gwyn [21] provided acceptable predictions in relation to the results observed in this paper.

REFERENCES

- [1] Freire, J.T, Ferreira, M.C, Freire, B.F, and Nascimento, B.S. (2012) A review on paste drying with inert particles as support medium. *Drying Technology*, **30**, 330- 341.
- [2] Markowski, M, Bialobrzewski, I, Modrzeska, A. (2010) Kinetics of spouted bed drying of barley: diffusivities for sphere and ellipsoid. *Journal of Food Engineering*. **96**, 380 – 387.
- [3] Rocha, S.C.S, Donida, M.W and Marques, A.M.M (2009) Liquid-particle surface properties on spouted bed coating and drying performance. *Canadian Journal of Chemical Engineering*, **87**, 695 – 703.
- [4] Borini, G.B, Andrade, T.C e Freitas, L.A.P (2009) Hot melt granulation of coarse pharmaceutical powders in a spouted bed. *Powder Technology*. **189**, 520 – 527.
- [5] Spiegl, N, Sivena, A, Lorente, E, Paterson, N. and Milian, M. (2010) Investigation of the Oxy-fuel gasification of coal in a laboratory-scale spouted bed reactor: reactor modifications and initial results. *Energy & Fuels*, **33**, 5281 – 5288.
- [6] Erkiaga, A, Lopez, G, Amutio, M, Bilbao, J, Olazar, M. (2014) Influence of operating conditions on the steam gasification of biomass in a conical spouted bed reactor. *Engineering Journal*, **237**, 259 – 267.
- [7] San José, M.J, Alvarez, S, Penãs, F.J. and García, I. (2014) Thermal exploitation of fruit tree pruning wastes in a novel conical spouted bed combustor. *Chemical Engineering Journal*, **238**, 227 – 233.
- [8] Amutio, M, Lopez, G, Artetxe, M, Elordi, G, Olazar, O, Bilbao, J. Influence of temperature on biomass pyrolysis in a conical spouted bed reactor. *Resources, Conservation and Recycling*, **59**, 23 – 31.
- [9] Elordi, G, Olazar, M, Lopez, G, Amutio, M, Artetxe, M, Aguado, R and Bilbao, J. (2009) Catalytic pyrolysis of HDPE in continuous mode over zeolite catalysts in a conical spouted bed reactor. *Journal of Analytical and Applied Pyrolysis*, **85**, 345 – 351.
- [10] Mathur, K.B e Epstein, N. (1974) *Spouted Beds*. Academic Press, New York.
- [11] Epstein, N e Grace, J. R. (1997) *Spouting of Particulate Solids – Handbook of Powder Science & Technology*. Chapman & Hall, New York. 531 – 567.
- [12] Epstein, N e Grace, J. R. (2011) *Spouted and Spout-Fluid Beds – Fundamentals and Applications*. Cambridge University Press Co., New York. 1 – 15.
- [13] Freire, J.T, (1992) Drying of pastes in spouted bed. In: Freire, J.T. e Sartori, D.J.M., Ed. *Special Topics in Drying*. Vol **1**. UFSCar, São Carlos, SP. 41-85. (In Portuguese).
- [14] Fernández-Akarregui, A, Malkibar, J, Alava, I, Diaz, L, Cueva, F, Aguado, R, Lopez, G, Olazar, M. (2012) Sand attrition in conical spouted beds. *Particuology*, **10**, 592 – 599.
- [15] Ray, Y.C e Jiang, T.S. (1987) Particle attrition phenomena in a fluidized bed. *Powder Technology*, **49**, 193 – 206.
- [16] Bemrose, C.R. e Bridgwater, J. (1987) A review of attrition and attrition test methods. *Powder Technology*, **49**, 97 – 126.
- [17] Flamant, G, Chraïbi, M. A, Vallbona, G, Bertrand, C. Decarbonation and attrition of calcite in a plasma spouted bed reactor. *Journal de Physique*, **51**, 527 – 534.
- [18] Massarani, G, Passos, M.L. and Barreto, W. Production of annatto concentrates in spouted beds. *The canadian journal of chemical engineering*, **70**, 954 – 959.
- [19] Al-Senawi, S, Hadi, B, Briens, C, Chabagno, J.M. (2008) A comparison of the breakage mechanisms for attrition of selected polymers in pneumatic transport and spouted beds. *International journal of chemical reactor engineering*. **6**, 1 – 46.
- [20] Lee, S.K, Jiang, X, Keener, T.C, Khang, S. J. (1993) Attrition of lime sorbents during fluidization in a circulating fluidized bed absorber. *Ind. Chem. Res.* **32**, 2758 – 2766.
- [21] Gwyn, J. E. (1969) On the particle size distribution function and the attrition of cracking catalyst. *AIChE Journal*, **15**, 35 – 39.
- [22] German, R.M. (1989) *Particle packing characteristics*. 1th Edition, Metal powder industries federation, Princeton, New Jersey. 121 – 130.
- [23] Narimatsu, C.P. (2004) Contributions to the study of drying in a vertical pneumatic bed. M.Sc. thesis, Federal University of São Carlos, Brazil, 2004. (In Portuguese).

NOMENCLATURE

$\overline{d_{ps}}$	Sauter average diameter	(mm)
\overline{P}	Average pressure	(kg/ms ²)
d_p	Particle diameter	(mm)
k_0	Kinect constant	(s ⁻¹)
k_1	Kinect constant	(m ² /s ²)
k_a	Attrition rate constant Lee's model	(s ⁻¹)
k_p	Constant model Gwyn	(s ^{-m})
M	Mass of the bed	(kg)
m	Exponent for time dependence of attrition	(-)
P	Pressure	(kg/ms ²)
R_t	Attrition rate	(kg/s)
t	Tempo	(s)
u	Air velocity	(m/s)
W	Mass of particulate materials	(kg)
X_a	attrition	(-)
x_i	Mass fraction	(-)
ρ	Particle density	(kg/m ³)
Greek symbols		
Θ	Sphericity	
Δ	Difference	
Subscript		
ap	apparent	
0	Initial	
t	tempo	
ms	Minimum spouting	
max	maximum	